[6]Fujimori, A., Wu, Z.-Y., Nikiforuk, P. N., and Gupta, M. M., "A Design of a Flight Control System Using Fuzzy Gain-Scheduling," *GNC Conference*, New Orleans, LA, 1997, pp. 1647–1653.

[7]Gahinet, P., Nemirovski, A., Laub, A. J., and Chilali, M., *LMI Control Toolbox*, The Math Works Inc., Natick, MA, May 1995.

Exoatmospheric Interceptor Pulse Motor Optimization with Discrete Bias Removal

Craig A. Phillips* and D. Stephen Malyevac†
U.S. Naval Surface Warfare Center, Dahlgren, Virginia 22448

Nomenclature

t	= time, s
t_g	= time-to-go to the intercept, s
t_{gmc}	= time-to-go to the intercept at the midcourse stage motor burnout (second pulse), s
$t_{\text{gmc min}}$	= minimum allowable time-to-go to the intercept at the midcourse stage motor burnout (second pulse), s
t_{mission}	= the total flight time to the intercept, s
t_{p1bo}	= flight time at burnout of first pulse, s
t_{rm}	= flight time at which the track bias is removed, s
t_2	= burn time of the second pulse, s
V_{MR1}	= average speed remaining to the intercept after midcourse stage first pulse burnout, m/s
ZEM_{BIAS}	= total zero effort miss value at current time due to the target track bias, m
ZEM_{31}	= total zero effort miss value at midcourse stage first pulse burnout, m
ZEM^*	= zero effort miss value at midcourse stage first pulse burnout due to all sources other than the track bias, m
ΔV_{2PUL}	= divert velocity of second pulse allowed for lateral maneuver, m/s
σ^2_{HE}	= variance of the total interceptor attitude navigation and control error, rad^2
σ^2_{VTGT}	= variance of the target velocity measurement error, $(\text{m/s})^2$

Introduction

In this Note, the problem of selecting the pulse split for a two-pulse motor of the exoatmospheric midcourse stage of a notional antitactical ballistic missile interceptor is considered. The pulse split reflects the fraction of total impulse allocated to each pulse. The midcourse stage operates outside the atmosphere during the long period between the separation of the final endoatmospheric stage and the separation of the kinetic kill vehicle (KKV), which contains a seeker and divert system for final homing. Reference 1 demonstrated the use of the mission chart approach for the analysis of these interceptors. This Note extends the methodology of Ref. 1 to include a large bias in the target track. A large bias in the track is defined as one that is greater than the ability of the KKV to correct. A bias in the target track process could be introduced by the following: 1) tracking and engaging the only visible object in the target complex that is not the desired target, 2) tracking all objects in a target complex but being unable to discriminate the desired target, or 3) attempting to engage an undetected object by estimating its states from other information. The bias in the target track is composed of both a position and a velocity component relative to the current true target kinematics. These two components of the error can be combined by extrapolating the velocity bias error through the time-to-go to intercept.

After the desired target and its state estimates are determined, the bias in the target track becomes apparent and the associated heading error is removed by diverting during the next propulsion burn.

Four scenarios are possible for removal of the bias in the target track. The underlying philosophy to these definitions is that for a successful intercept each pulse must be able to remove all of the zero effort miss (3σ value) present at its ignition. The first scenario is defined by the removal of the bias during the first or second pulse burn. Because of the short burn times relative to the mission times, only a relatively small portion of the intercept population will fall under this category, and therefore this scenario is deemed inappropriate for consideration in the pulse split optimization. The second scenario is defined by the removal of the bias before the ignition of the first pulse. This scenario can affect mission timelines but is not a driver in the pulse split optimization. The third scenario is defined by the removal of the bias after the second pulse burn. In this situation, the zero effort miss from the bias in the target track must be removed entirely by the KKV divert. For large biases in the target track greater than the KKV divert, such a mission is infeasible. Modification of the pulse split provides no benefit in this scenario and shall not be pursued. The fourth scenario is defined by the removal of the bias in the target track between the burnout of the first pulse and the ignition of the second pulse. One of the primary uses of a two-pulse motor is to delay the ignition of the second pulse until after the bias in the target track is removed. This last scenario is of greatest operational interest and has the greatest impact on the optimization of the pulse motor.

The remainder of the Note will concentrate on the optimization of the pulse motor for this fourth scenario. The changes to the second pulse timeline constraints when a large bias in the target track is introduced in this scenario are presented. The impact of the pulse split on the requirements placed on the weapon system timeline for removal of the bias in the target track will be demonstrated. Finally, the relationship of the maximum and minimum feasible mission times to the pulse split is discussed for this scenario.

Second Pulse Timeline Constraints in the Presence of a Bias

Reference 1 defined five constraints on the second pulse ignition and burnout timeline. When the bias in the target track is removed between the two pulses, only the minimum time-to-go at the second pulse burnout constraint changes relative to the definition in Ref. 1. The bias in the target track must be included in the errors at first pulse burnout that the second pulse must remove. The errors at second pulse burnout are not affected by the bias in the target track because the scenario defines them as removed by the second pulse.

The magnitude of the bias is considered fixed for this analysis, but its spatial orientation could vary considerably. A conservative approach is used in that the zero effort miss (ZEM) from the bias in the target track is "stacked" with the ZEM from the nominal error tree by assuming they are aligned. Although not strictly correct, it adds another degree of conservatism to the analysis. In this approach, the ZEM at first pulse burnout is given by

$$3\sigma\text{ZEM}_{31} = 3\sigma\text{ZEM}^* + \text{ZEM}_{\text{BIAS}} \tag{1}$$

For a successful intercept, the second pulse must be able to remove all of the zero effort miss (3σ value) present at the first pulse burnout. This requirement determines the minimum allowable time-to-go from second pulse burnout to the intercept. The minimum time-to-go expressed by

$$t_{\text{gmc min}} \approx \frac{3\left(\sigma^2_{\text{HE}} V^2_{\text{MR1}} + \sigma^2_{\text{VTGT}}\right)^{\frac{1}{2}}(t_{\text{mission}} - t_{\text{p1bo}}) + \text{ZEM}_{\text{BIAS}}}{\Delta V_{\text{2PUL}}} \tag{2}$$

Received 1 April 1999; revision received 24 August 1999; accepted for publication 25 August 1999. This material is declared a work of the U.S. Government and is not subject to copyright protection in the United States.

*Lead Functional Design Engineer, Missile Systems Engineering Branch, Weapons Systems Department, Dahlgren Division, G23, 17320 Dahlgren Road. Senior Member AIAA.

†Lead Functional Design Engineer, Missile Systems Engineering Branch, Weapons Systems Department, Dahlgren Division, G23, 17320 Dahlgren Road. Member AIAA.

Pulse Split and Latest Time for Bias in the Target Track Removal

The pulse split drives the minimum time-to-go at the second pulse burnout constraint. This minimum time-to-go determines the latest time for second pulse ignition and the latest feasible time for the bias in the target track to be removed for a successful mission.

For a numerical example, the interceptor parameters from Ref. 1 and the high-quality error set from that reference will be used. Both an 80/20- and a 50/50-pulse split will be considered. The 80/20-pulse split has 80% of the impulse in the first pulse and 20% in the second pulse. The 50/50 split has 50% of the total impulse in the first pulse and 50% in the second pulse.

The mission chart in Fig. 1 shows the effect of using the second pulse to remove a target track bias ZEM of 7.5 km for the two midcourse-stage pulse splits considered. The minimum time-to-go at second pulse burnout constraint [Eq. (2)] yields a separate minimum time-to-go at the second pulse burnout constraint for each pulse split. This constraint then determines the latest time that the track bias may be removed for a successful intercept:

$$t_{\text{rm}} \leq t_{\text{mission}} - (t_{\text{gmc min}} + t_2) \tag{3}$$

Figure 2 shows this value as a function of the mission time for the 50/50- and 80/20-pulse split motors. The use of the 50/50 motor relaxes the required track quality of the weapon system by allowing bias in the target track to be removed later in the mission.

Pulse Split and Feasible Mission Times

The pulse split also drives the maximum and minimum feasible mission times. Because of error and divert considerations, an interceptor design may not be able to fully use all of its kinematic capability as indicated by its kinematic limit. Point D in Fig. 1 indicates the maximum feasible mission for the 50/50-pulse split. This point represents the intersection of the minimum time-to-go at second pulse burnout constraint [Eq. (2)] and the 50/50-interceptor kinematic mission time limit. For this pulse split, missions up to the kinematic limit of 425 s are possible. The maximum feasible mission for the 80/20-pulse split is determined from the intersection of the minimum and maximum time-to-go at second pulse burnout constraints (point B in Fig. 1). This intersection results in a maximum mission time of 317 s. Error and divert considerations prevent the 80/20 missile from flying intercepts out to the maximum possible flight time as given by the 80/20 kinematic limit. Thus, the 80/20 missile is being limited by an error derived mission time limit, whereas the 50/50 missile is limited by its kinematic limit.

The choice of pulse split drives not only the maximum mission time but also the minimum mission time. The 50/50-pulse split allows use of missions down to the shortest time dictated by the minimum KKV homing time. Point E indicates this shortest feasible mission as 81 s in Fig. 1. This point is defined by the intersection of the sequencing limit and the minimum time-to-go constraint for the second pulse burnout dictated by the KKV minimum homing time. The 80/20-pulse split does not allow missions less than 110 s. This limit is determined from the intersection of the sequencing limit and the 80/20 minimum time-to-go at the second pulse burnout constraint [Eq. (2)]. This intersection is marked as point C in Fig. 1. By requiring longer minimum mission times, the 80/20-pulse split interceptor could create a hole in the engagement space above the interceptor launch point.

Table 1 summarizes the minimum and maximum mission times for each pulse split when the kinematic capabilities, errors, and divert capabilities are considered.

Table 1 Feasible mission limits

Interceptor pulse split	Minimum feasible mission, s	Maximum feasible mission, s
50/50	81	425
80/20	110	317

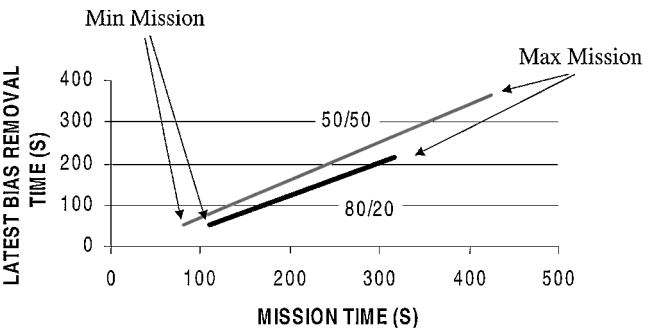

Fig. 2 Latest bias removal time.

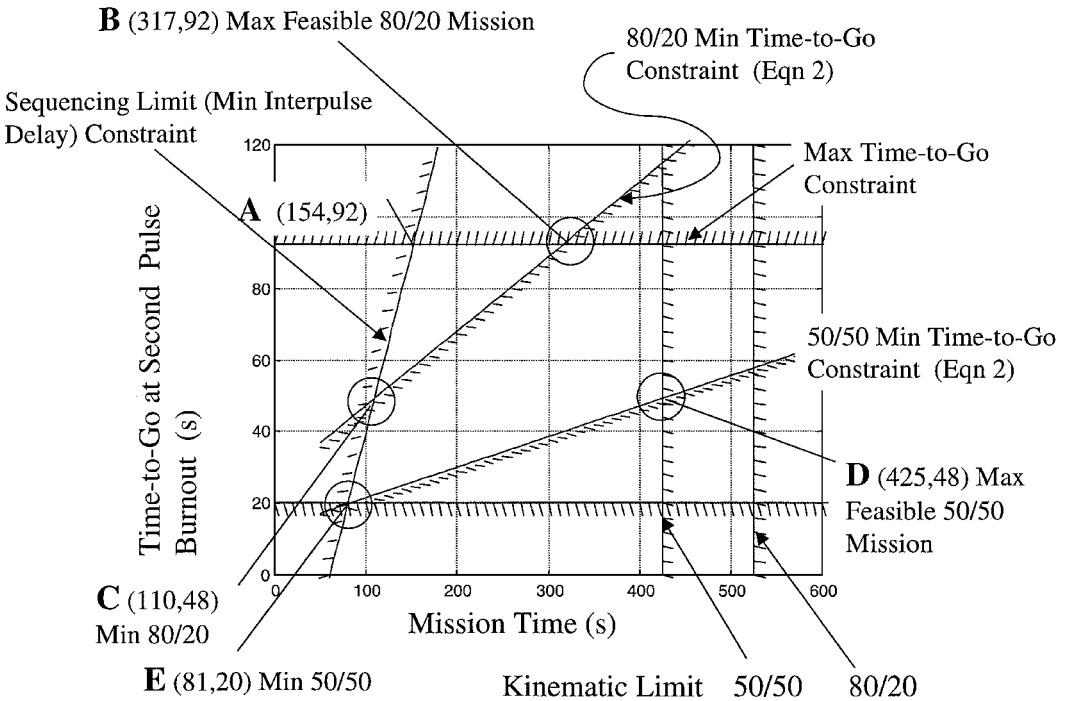

Fig. 1 Mission chart for two pulse splits.

Conclusions

These results demonstrate that the use of larger second pulse fractions in the presence of a large bias in the track (that is, greater than the KKV divert) can reduce the requirements on the weapon system by allowing the bias in the target track to be removed later during the flight. Additionally, the 50/50-pulse split extends both the minimum and maximum feasible mission times relative to the 80/20-pulse split. This increases the engagement envelope of the interceptor in the presence of a large bias in the target track.

Reference

[1]Phillips, C. A., and Malyevac, D. S., "Pulse Motor Optimization via Mission Charts for an Exoatmospheric Interceptor," *Journal of Guidance, Control, and Dynamics*, Vol. 21, No. 4, 1998, pp. 611–617.

Nonlinear Entry Trajectory Control Using Drag-to-Altitude Transformation

Shinji Ishimoto*
National Aerospace Laboratory, Chofu, Tokyo 182-8522, Japan

I. Introduction

EXISTING entry guidance systems are based on the common concept of tracking a reference drag profile. For that purpose, trajectory control laws are incorporated into the guidance systems. A linear control law has been employed successfully for the Space Shuttles.[1] This control law was designed with a classical method based on linearized equations of motion. This approach generally needs gain schedules interpolating feedback gains selected at individual design points. However, it is not an easy task to prepare such gain-scheduling functions that give a satisfactory performance over the whole entry phase. Motivated by this fact, many authors recently have proposed nonlinear trajectory control laws.[2–5] These control laws were developed with the feedback linearization (or dynamic inversion) method[6] or related methods. Design parameters of these techniques are some constants describing a desired response independent of reference values. Therefore, extensive gain schedules are not necessary. For this reason, nonlinear control laws will be the mainstream for entry guidance in place of linear control laws. A new nonlinear control law is proposed using a device called the altitude-to-drag transformation. The altitude instead of the drag force is considered as the controlled variable. The new nonlinear control law is described and numerically compared with a conventional linear control law.

II. Nonlinear Trajectory Control Law

A. Basic Control Law

The primary function of entry trajectory control laws is to modulate the bank angle (roll angle around the atmospheric-relative velocity). The control law proposed in the note is summarized as

$$\ddot{h}_C = \ddot{h}_{\mathrm{REF}} + f_1 h_{\mathrm{ERR}} + f_2 \dot{h}_{\mathrm{ERR}} + f_3 \int h_{\mathrm{ERR}}\, \mathrm{d}t \tag{1}$$

$$(L/D)_C = \ddot{h}_C/D + \dot{h}/V + (g/D)(1 - V^2/V_S^2) \tag{2}$$

$$\phi_C = \cos^{-1}\left[\frac{(L/D)_C}{L/D}\right] \tag{3}$$

Received 14 June 1999; presented as Paper 99-4169 at the AIAA Atmospheric Flight Mechanics Conference, 9–11 August 1999; revision received 26 September 1999; accepted for publication 30 September 1999.

*Senior Researcher, Flight Research Division, 7-44-1 Jindaijihigashi-machi. Member AIAA.

where D is the drag force per unit mass (also termed drag acceleration), g is the acceleration due to gravity, h is the altitude, $\dot{h}$ is the altitude rate, $\ddot{h}$ is the vertical acceleration, L/D is the lift-to-drag ratio, V is the Earth-relative velocity, V_S is the circular orbital velocity, and ϕ is the bank angle. The subscripts C, ERR, and REF stand for a command, an error, and a reference value, respectively. The symbols without any subscripts denote real-time measurements. The feedback gains, f_1, f_2, and f_3, characterize the desired vertical acceleration $\ddot{h}_C$ for attenuating the altitude error h_{ERR}. The intermediate lift-to-drag ratio command $(L/D)_C$ is a normalized version of the vertical component of lift force required for trajectory control. The mapping function (2) is based on the following equation of motion in the vertical direction

$$\ddot{h} = -D(\dot{h}/V) + L\cos\phi - (g/D)\left[1 - (V^2/V_S^2)\right] \tag{4}$$

where L is the lift force per unit mass. Correspondence between Eqs. (2) and (4) is obvious, since $L\cos\phi$ in Eq. (4) represents the vertical component of lift force.

B. Tracking Error

The errors used in the control law (1) are defined as

$$h_{\mathrm{ERR}} = h_{\mathrm{REF}} - h_D \tag{5}$$

$$\dot{h}_{\mathrm{ERR}} = \dot{h}_{\mathrm{REF}} - \dot{h} \tag{6}$$

where h_D is a pseudo-altitude derived from the drag acceleration, and $\dot{h}$ is an altitude rate estimated by a navigation system. The reference altitude h_{REF} and the drag-derived altitude h_D are computed from the common models for the drag force and atmospheric density

$$D = \left[\rho V^2 S C_D(V)\right]/2m \tag{7}$$

$$\rho = \rho_0 \exp(-h/h_S) \tag{8}$$

where C_D is the drag coefficient, h_S is the atmospheric density scale height, m is the vehicle mass, S is the vehicle reference area, ρ is the atmospheric density, and ρ_0 is the atmospheric density at sea level. In general, C_D is a function of the angle of attack α and the Mach number. However, the atmospheric-relative velocity is almost equal to V, and the speed of sound is nearly constant during entry. In addition, we assume that α is scheduled as a function of V. Therefore, C_D is described as a function of only V as shown in Eq. (7).

When the reference drag D_{REF} is a function of the specific energy (energy per unit mass) E, the altitude error h_{ERR} is explicitly written as

$$h_{\mathrm{ERR}} = -h_S[\log(D_{\mathrm{REF}}/D)]W_2 \tag{9}$$

$$W_1 = 1 + (V/2)(C_D'/C_D) \tag{10}$$

$$W_2 = \left[1 + (2gh_S/V^2)W_1\right]^{-1} \tag{11}$$

where C_D' represents $\partial C_D/\partial V$. If D_{REF} is a function of V, we do not need W_2 in Eq. (9). The scale height h_S is generally scheduled as a function of the altitude based on a standard atmosphere. Equation (9) can be derived from Eqs. (7) and (8) by using the relation:

$$E = \tfrac{1}{2}V^2 + gh = \tfrac{1}{2}V_{\mathrm{REF}}^2 + gh_{\mathrm{REF}} \tag{12}$$

and the assumption $gh_{\mathrm{ERR}} \ll V^2$, which usually holds during entry.[7]

Linearizing Eq. (9) about D_{REF}, we obtain the following expression:

$$h_{\mathrm{ERR}} \cong -h_S(W_2/D_{\mathrm{REF}})(D_{\mathrm{REF}} - D) \tag{13}$$

If this formula is adopted for mapping the drag error into h_{ERR}, the control law as shown in Eq. (1) becomes equivalent to a conventional linear control law.[1] Equation (13) implies that the scale height h_S works as a part of the feedback gain with respect to the drag error. The inaccuracy of h_S included in the reference altitude rate $\dot{h}_{\mathrm{REF}}$ (the definition is shown later) causes a steady-state tracking error, but this error is eliminated by the integral term in Eq. (1). Therefore,